Mutant ubiquitin-mediated β-secretase stability via activation of caspase-3 is related to β-amyloid accumulation in ischemic striatum in rats

Yong Zhang[1], Man Xiong[1], Ri-Qiang Yan[2] and Feng-Yan Sun[1]

[1]Department of Neurobiology, Institute of Biomedical Sciences, State Key Laboratory of Medical Neurobiology, Shanghai Medical College of Fudan University, Shanghai, People's Republic of China; [2]Department of Neuroscience, Lerner Research Institute, Cleveland Clinic, Cleveland, Ohio, USA

Previous studies have demonstrated that ischemic stroke increases β-amyloid (Aβ) production by increasing β-secretase (BACE1) through activation of caspase-3, and stimulates generation of mutant ubiquitin (UBB^{+1}) in rat brains. In this study, we examined whether caspase-3 activation participates in the regulation of UBB^{+1} generation and UBB^{+1}-mediated BACE1 stability in ischemic injured brains. The results showed that UBB^{+1} and activated caspase-3-immunopositive-stained cells were time dependently increased in the ipsilateral striatum of rat brains after middle cerebral artery occlusion. UBB^{+1}-immunopositive cells could be co-stained with caspase-3, Aβ (UBB^{+1}–Aβ), and BACE1 (UBB^{+1}–BACE1). BACE1 protein could also be pulled down by immunoprecipitation with UBB^{+1} antibody. Z-DEVD-FMK (DEVD), a caspase-3 inhibitor, significantly decreased the level of UBB^{+1} protein and the number of UBB^{+1}–Aβ and UBB^{+1}–BACE1 double-stained cells in the ischemic striatum, as well as the level of UBB^{+1}/BACE1 protein complex. We conclude that activation of caspase-3 might be upstream of UBB^{+1} formation and that excessive UBB^{+1} could bind to BACE1 and increase the stability of BACE1, thereby increasing Aβ in ischemic injured brains. These results suggest new biological and pathological effects of caspases and regulation of the ubiquitin–proteasome system in the brain. Our results provide new therapeutic targets to prevent further neurodegeneration in patients after stroke.

Introduction

Stroke is a primary cause of disability in humans. In particular, cognitive function can be attenuated or even lost within 3 years after ischemic stroke, which occurs in about 30% of stroke patients (Leys *et al*, 2005). The pathological mechanisms of ischemic neuronal death or degeneration are very complex. It has been shown that a transient cerebral ischemia can significantly increase β-amyloid (Aβ) generation, a main component of senile neuritic plaques, by activation of β-secretase (BACE) and γ-secretase in the brain, both of which are Aβ-synthetic enzymes (De Strooper *et al*, 1998; Sinha *et al*, 1999; Vassar *et al*, 1999; Xiong *et al*, 2008; Yan *et al*, 1999). This change might be

associated with the occurrence of post-stroke dementia in diabetic and normal rats (Xiong *et al*, 2008; Zhang *et al*, 2009). Activation of caspase-3, a key enzyme of the caspase-dependent apoptotic pathway, also triggers Aβ generation through increases in the amount and activity of BACE1, as we have found that a caspase-3 inhibitor blocks ischemia-induced BACE1 activation and Aβ accumulation in rat brains (Xiong *et al*, 2008). Activation of BACE1 is positively related to the amount of BACE1 protein. Therefore, the balance between BACE1 synthesis and degradation determines the level of BACE1 activity in the brain. Degradation of BACE1 depends on several pathways, including the ubiquitin–proteasome system (UPS) (Qing *et al*, 2004). However, whether and how ubiquitin-mediated BACE1 degradation is involved in the pathogenesis of ischemic injured brains, remains to be determined.

Normal function of the UPS in the brain is very important for maintaining neurotransmission, neural plasticity, and cell viability (Ciechanover and Brundin, 2003). It has been shown that UPS

dysfunction occurs in the brains of patients with Alzheimer's disease (Lopez Salon et al, 2000) and ischemic stroke (Keller et al, 2000). Cerebral ischemia results in impairment of the UPS (Bence et al, 2001), including reduction of proteasomal activity (Kamikubo and Hayashi, 1996; Keller et al, 2000), depletion of ubiquitin (Morimoto et al, 1996), and upregulation of mutant ubiquitin UBB^{+1}, which comprises a ubiquitin moiety and a 19-aa C-terminal extension (Yamashiro et al, 2007). UBB^{+1} was first discovered as a component of tau pathology in Alzheimer's disease and Down's syndrome (van Leeuwen et al, 1998). Under physiological conditions, UBB^{+1} exists in the brain at low levels and can be polyubiquitinated (De Vrij et al, 2001; Lam et al, 2000; Lindsten et al, 2002) and degraded by the proteasome as an enzyme substrate (Lindsten et al, 2002). However, at high levels, UBB^{+1} becomes a potent competitive inhibitor of proteasome activity and plays an inhibitory role in the function of the UPS (van Tijn et al, 2007). Therefore, excessive UBB^{+1} in the tissues has been proposed to represent an endogenous readout of proteasomal dysfunctions (Fischer et al, 2003; Hol et al, 2005). In a transient global ischemia model, UBB^{+1} can be selectively accumulated in hippocampal CA1 pyramidal neurons, where neurons express caspase-3 at an earlier stage of the pathological process following brain ischemia and subsequently proceed to apoptosis at a later stage (Chen et al, 1998). Our previous results showed that inhibition of caspase-3 activation attenuates Aβ generation by reduction of BACE1 production and activity in rat brains after stroke (Xiong et al, 2008). As mentioned above, BACE1 can be ubiquitinated and degraded by the proteasome. However, it is still unknown whether caspases modulate ubiquitin-mediated BACE1 degradation in ischemic rat brains.

In this study, we examined active caspase-3 and mutant ubiquitin UBB^{+1} in rat brains following transient middle cerebral artery occlusion (MCAO) and the effects of caspase-3 on the interaction of UBB^{+1} with BACE1. We found that cerebral ischemia time-dependently increased UBB^{+1}, which was later than that of caspase-3. Cellular distribution showed that UBB^{+1} colocalized with caspase-3 and BACE1/Aβ in astrocytes. Inhibition of caspase-3 activity attenuated the ischemia-induced increase of UBB^{+1} protein and the interaction between UBB^{+1} and BACE1 proteins, thereby decreasing Aβ in rat brains after ischemia. These results indicate new biological and pathological effects of caspase and UPS regulation in the brain. The results present also provide new therapeutic targets for preventing further neurodegeneration in patients after stroke.

Materials and methods

Ischemia Procedure and Administration of Z-DEVD-FMK

Male Sprague–Dawley rats (220 to 250 g) were purchased from the Shanghai Experimental Animal Center of the Chinese Academy of Sciences. The Medical Experimental Animal Administrative Committee of Shanghai approved all the experiments. All rats were habituated to the colony and had free access to laboratory chow and water prior to experimental procedures. Before surgery, animals were anesthetized with 10% chloral hydrate (360 mg/kg, intraperitoneal), and arterial blood pO$_2$, pCO$_2$, and pH were monitored using an AVL 990 Blood Gas Analyzer (AVL Co., Graz, Austria). Rectal temperature was maintained at 37 ± 0.5°C with a temperature-regulated heating lamp. Rats were subjected to transient focal cerebral ischemia induced by left MCAO, according to procedures described previously (Qiu et al, 2003; Wang et al, 2007). Briefly, a 4-0 nylon monofilament suture with a rounded tip was gently advanced into the internal carotid artery for a distance of about 22 mm from the common carotid artery bifurcation, to occlude MCA blood flow. During the process of ischemia, we used a laser Doppler perfusion monitor (Periflux system 5000; Perimed AB, Järfälla, Sweden) to detect blood flow in the trunk of MCA synchronously. The blood flow dropped to < 20% of the baseline, denoting that the MCA block was successful. After 30 mins of occlusion, the suture was withdrawn and blood flow was restored. For drug treatments, rats were injected intracerebroventricularly with either Z-DEVD-FMK (DEVD, purchased from Alexis Biochemicals, Grünberg, Germany) or vehicle, according to a procedure described previously (Chen et al, 1998; Xiong et al, 2008). Briefly, each animal received three ventricular infusions of 10 µL of vehicle or DEVD (1.5 µg/µL) each over a 20-min time period, 30 mins prior to MCAO, and then received two additional infusions at 2 and 24 h following MCAO. After operation, the rats were returned to the cage and had free access to food and water. For the time-course analysis, rats were killed at 1, 3, 7, and 14 days after MCAO. For the remaining studies, the rats were killed at 7 days after MCAO.

Tissue Preparation and Immunohistochemistry

Rats were killed with an overdose of 10% chloral hydrate. The brains were removed and coronal sections were cut with a freezing microtome (Jung Histocut, model 820-II; Leica, Nussloch, Germany) at a thickness of 30 µm at Bregma levels ranging from 1.60 to −4.80 mm. Sections were stored at −20°C in a cryoprotectant solution for histological analysis.

Immunohistochemical staining was performed as described previously (Xiong et al, 2008; Zhang et al, 2009). The sections were incubated with rabbit polyclonal anti-UBB^{+1} (Ubi2a, epitope: RQDHHPGSGAQ; Upstate Biotechnology, Lake Placid, NY, USA; 1:400 dilution) or rabbit anti-activated caspase-3 antibody (Abcam, Cambridge, UK; 1:20 dilution) overnight at 4°C. After the unbound primary antibodies were removed, the sections were incubated with the corresponding biotinylated secondary antibodies (1:200 dilution) for 45 mins at 37°C, followed by avidin–biotin peroxidase for 45 mins at 37°C (Vectastatin Elite ABC kit; Vector Laboratories Inc., Burlingame, CA, USA; 1:200 dilution). Immunoreactivity was visualized with 0.05% diaminobenzidine in Tris-HCl buffer (0.1 mol/L, pH 7.6) containing 0.03% H$_2$O$_2$, or

developed using a VectorBlue kit (blue color, Vectastatin Elite ABC kit; Vector Laboratories Inc., Burlingame, CA, USA) in Tris-HCl buffer (0.1 mol/L, pH 8.2), respectively. Negative control sections received identical treatment except for the primary antibody, and showed no positive signal.

For UBB^{+1} and glial fibrillary acidic protein (GFAP), NeuN, or caspase-3 double fluorescence immunostaining, the sections were incubated with rabbit polyclonal anti-UBB^{+1} antibody (1:400 dilution) and mouse monoclonal anti-GFAP antibody (NeoMarker, Fremont, CA, USA; 1:200 dilution) or mouse monoclonal anti-NeuN antibody (Sigma, St Louis, MO, USA; 1:200 dilution), or rabbit polyclonal anti-activated caspase-3 antibody (1:20 dilution) at 4°C, overnight. Sections were then incubated with anti-rabbit IgG-fluorescein isothiocyanate (Santa Cruz Biotechnology, Santa Cruz, CA, USA; 1:40 dilution) and anti-mouse or anti-rabbit IgG–rhodamine (Roche, Mannheim, Germany, 1:40 dilution) at 37°C for 45 mins to reveal the positive signals.

For triple staining of caspase-3, UBB^{+1}, and Aβ_{x-42}, the sections were incubated with rabbit polyclonal anti-activated caspase-3 antibody (1:20 dilution) at 4°C, overnight. After rinsing in phosphate-buffered saline, the sections were incubated with anti-rabbit IgG–rhodamine (1:40 dilution) at 37°C for 45 mins and then with rabbit polyclonal anti-UBB^{+1} antibody (1:400 dilution) and mouse monoclonal anti-Aβ_{x-42} (Upstate, NY, USA; 1:100 dilution) at 4°C, overnight. Sections were then incubated with anti-rabbit IgG–fluorescein isothiocyanate (1:40 dilution) and anti-mouse IgG–Cy5 (Amersham Pharmacia Biotechnology, Buckinghamshire, UK; 1:200 dilution) at 37°C for 45 mins. For triple staining of caspase-3, UBB^{+1}, and BACE1, the sections were reacted with BACE1 antibody (Calbiochem, Darmstadt, Germany; 1:100 dilution) after immunostaining with caspase-3 and UBB^{+1}, and the signals were then revealed by anti-rabbit IgG–Cy5 under the above conditions. After washing, the sections were mounted on glass slides and coverslipped using fluorescence mounting medium (Vector Laboratories, Burlingame, CA, USA). Fluorescence was detected at an excitation wavelength of 650 nm and emission detection wavelengths of 670 (Cy5); 535 and 565 nm (rhodamine); and 490 and 525 nm (fluorescein isothiocyanate) by confocal laser-scanning microscopy (TCS SP2; Leica, Mannheim, Germany).

Immunoblotting and Immunoprecipitation

Rat striatum was homogenized in radioimmunoprecipitation assay buffer (1× phosphate-buffered saline, 1% Nonidet P-40, 0.5% sodium deoxycholate, 0.1% sodium dodecyl sulfate, and 1 mmol/L sodium orthovanadate) containing a protease inhibitor cocktail (Roche, Basel, Switzerland). Protein lysates were obtained after centrifugation at 12,000*g* for 30 mins. Protein concentration was determined using a Bio-Rad protein assay. Equal amounts of protein lysates were separated on 8% or 12% sodium dodecyl sulfate–polyacrylamide gels and electrophoretically transferred onto polyvinylidene difluoride mem-

branes. The membranes were incubated with rabbit polyclonal anti-UBB^{+1} antibody (Upstate Biotechnology, Lake Placid, NY, USA; 1:2000 dilution) or rabbit polyclonal anti-BACE1 (1:1000 dilution) or rabbit polyclonal anti-caspase-3 (Santa Cruz Biotechnology, Santa Cruz, CA, USA; 1:200 dilution), which recognizes both full-length and cleaved fragments of caspase-3, at 4°C, overnight, and then with horseradish peroxidase-conjugated anti-rabbit IgG (1:3000 dilution). The immunoreactivity was visualized by enhanced chemiluminescence substrate system (ECL). Normalization was achieved by stripping filters and reprobing for β-actin. Films were scanned and subsequently analyzed by measuring the optical densities of immunostained bands using an image-processing and analysis system (Bio-Rad, Hercules, CA, USA).

For immunoprecipitation, the lysates were incubated with a primary capturing antibody, rabbit polyclonal anti-UBB^{+1} (Upstate Biotechnology, Lake Placid, NY, USA) or rabbit polyclonal anti-BACE1, at 4°C, overnight, and with protein A beads at 4°C for 2 h. The protein–antibody complexes were isolated and the immunoprecipitates were then analyzed on 8% sodium dodecyl sulfate–polyacrylamide gels using the detecting antibody, rabbit polyclonal anti-BACE1 (1:1000 dilution) or polyclonal anti-UBB^{+1} (1:2000 dilution) for co-immunoprecipitation, respectively.

Data Quantification and Statistical Analysis

For immunostaining, brain sections were observed under a light microscope and used for quantification of the number of striatal cells positive for UBB^{+1} or caspase-3 using an image-processing and analysis system (ImageJ 1.37 software; NIH, USA). The numbers of UBB^{+1}–BACE1, UBB^{+1}–Aβ double-stained cells and UBB^{+1}–BACE1–caspase-3, UBB^{+1}-Aβ-caspase-3 triple-stained cells were counted on the basis of the method described in our previous report (Xiong *et al*, 2008). Four confocal images (with a fixed thickness of 15 μm) were acquired randomly per section in the peri-ischemic striatum under a ×40 object lens of a confocal laser-scanning microscope, and then double- or triple-labeled cells were counted manually. The double- or triple-labeled cells in each section are the average number from four images and are expressed as cells/mm^2.

All data are expressed as mean ± s.e.m. Multiple groups were compared by one-way analysis of variance followed by LSD test. Comparison between two experimental groups was made by unpaired Student's *t*-test. Statistical significance was set at $P < 0.05$.

Results

Cerebral Ischemia Increased UBB^{+1} in Astrocytes in Rat Striatum

In this study, a 30-mins MCAO was used to induce focal cerebral ischemia. We observed that ischemic infarct core mainly located in the lateral striatum and near cortex, which was consistent with our previous reports (Hou *et al*, 2008; Xiong *et al*, 2008). Using this MCAO model, we determined whether UBB^{+1}
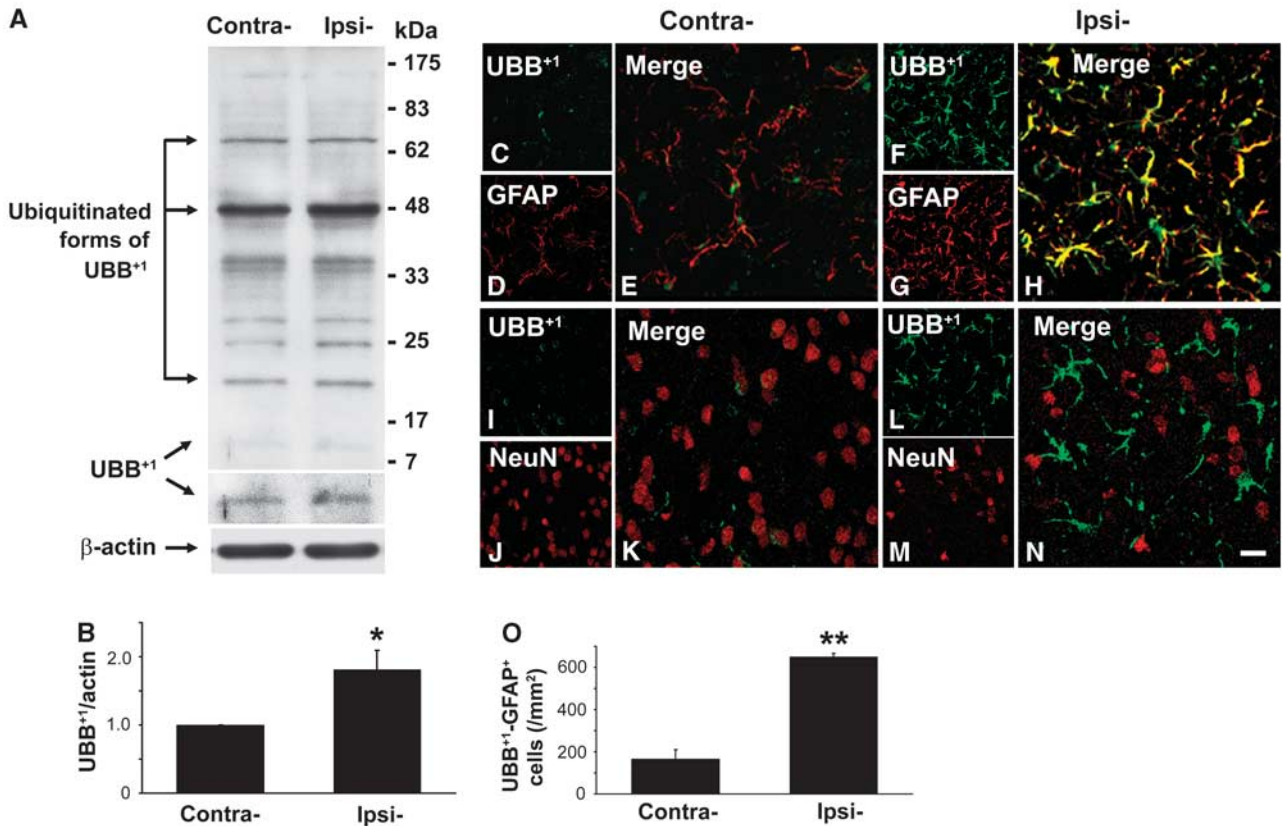
Figure 1 Changes in the expression of UBB^{+1} in the ischemic striatum of rats. Western blots of treated brain lysates showed elevated levels of UBB^{+1} protein (11 kDa) in the ipsilateral (Ipsi-) striatum 7 days after MCAO as compared with the contralateral (Contra-) striatum (**A**, **B**). Immunofluorescent double staining revealed elevated UBB^{+1}-positive signals markedly to co-localize with GFAP$^+$ signals in the ipsilateral ischemic striatum (**F–H**), and few UBB^{+1}-positive signals to co-label with NeuN$^+$ signals (**L–N**). UBB^{+1}-positive signals in the contralateral striatum were much weaker (**C–E**, **I–K**). Scale bars: 20 μm. Quantitative analysis of UBB^{+1}–GFAP$^+$ cells (**O**) is shown graphically as mean ± s.e.m. (*$P < 0.05$ versus contralateral; **$P < 0.01$ versus contralateral; $n = 3$ to 4 in each group).

formation was involved in the pathological process of rat brain after cerebral ischemic injury. Therefore, we measured the protein level of UBB^{+1} in both contralateral and ipsilateral striatum of rat brains by western blotting. Figure 1A shows the presence of unmodified UBB^{+1} as well as several high-molecular-weight bands. This pattern corresponds to that found in earlier studies in which the bands were identified as conjugates of UBB^{+1} with ubiquitin moieties (De Vrij et al, 2001; Lam et al, 2000). We found that the protein level of UBB^{+1} was significantly elevated in the ipsilateral striatum of rat brain at 7 days after MCAO as compared with that in the contralateral striatum to ischemia (Figure 1B).

Next, we investigated the cellular localization of UBB^{+1} in ischemic rat brain by confocal microscopy. In ischemic striatum of rat brain, UBB^{+1}-positive stained cells were mainly astrocytes, since most of them showed positive immunostaining for GFAP, an astrocyte marker, and showed astrocyte morphology (Figure 1F–1H). Only a few UBB^{+1}-positive stained cells were co-labeled with NeuN, a neuronal marker, in the ipsilateral striatum (Figure 1L–1N).

However, in the contralateral striatum, the immunofluorescence signal for UBB^{+1} was much weaker both in astrocytes and neurons (Figure 1C–1E and 1I–1K). The cell counting results showed that the number of UBB^{+1}–GFAP double-stained cells in the ipsilateral striatum at 7 days after MCAO increased to 649.8 ± 16.2 cells/mm^2, compared with 166.5 ± 44.0 cells/mm^2 in the contralateral striatum (Figure 1O).

Cerebral Ischemia Time-Dependently Increased UBB^{+1} and Active Caspase-3 in Rat Striatum

Rats were subjected to 30-min MCAO and killed 1, 3, 7, or 14 days after ischemia–reperfusion. In this study, we found that UBB^{+1}-positive stained cells were detected in ischemic striatum and elevated in a time-dependent manner (Figure 2A–2C). Consistent with above results, most UBB^{+1}-positive stained cells appeared in the astrocytes, which were mainly distributed in the dorsal- and ventral-medium parts of striatum around ischemic core (the peri-ischemic striatum) at 7 days after MCAO. The number of UBB^{+1}-positive stained cells was counted in the
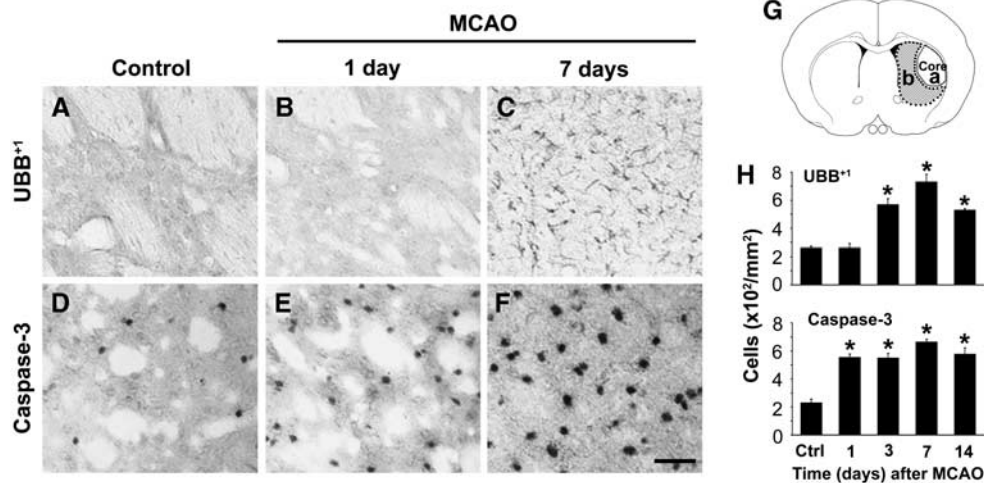
Figure 2 Time-dependent increase of UBB $^{+1}$ and active caspase-3 in the striatum of rats after ischemia. Brain sections from rats killed at 1, 3, 7, and 14 days after MCAO were immunostained with UBB $^{+1}$ (**A**–**C**) and active caspase-3 (**D**–**F**). Scale bars: 50 μm. Diagram **G** illustrates the area of the ischemic infarct core (dotted line, a) and the region for immunostaining observation (shade area, b). Cell counting and statistical analysis showed time-dependent increase in UBB $^{+1}$ (**H**, upper) and active caspase-3 (**H**, lower) immunoreactivity in the ischemic striatum of rat brains (mean ± s.e.m.; *$P < 0.05$ versus normal control rats (Ctrl/control); $n = 3$ to 4 in each group).

peri-ischemic striatum, as indicated in Figure 2G-b. The results showed that UBB $^{+1}$-positive stained cells began to increase in the ischemic striatum of rats at 3 days after MCAO as compared with that in normal control rats (control), reached its peak at 7 days, and then slightly diminished at 14 days after ischemia (Figure 2H).

We also found that immunostained cells with active form of caspase-3, a key enzyme in the apoptotic signaling pathway, were clearly increased in the ischemic striatum of rat brains as early as 1 day after MCAO, which appeared earlier than UBB $^{+1}$ formation, and further increased at 7 days, with higher density of nucleus positive staining of active caspase-3 $^{+}$ (Figure 2D–2F). Quantitative analysis further indicated that activated caspase-3 $^{+}$ cells in the ipsilateral striatum to MCAO also elevated in a time-dependent manner (Figure 2H).

UBB $^{+1}$ Colocalized with Activated Caspase-3 in Ischemic Striatum of Rat Brain

To determine whether elevated levels of UBB $^{+1}$ and active caspase-3 occurred in the same cells within the striatum of ischemic rat brain, we performed double immunostaining of UBB $^{+1}$ and active caspase-3 combined with confocal microscopy in brain sections from rats at 7 days after MCAO. In this study, we found that most UBB $^{+1}$-positive stained cells co-labeled with active caspase-3 (Figure 3A–3D). The confocal microscopy examination showed that UBB $^{+1}$-positive signals were distributed not only in the cytoplasm of astrocytes, but also in the nucleus, where they co-stained with active caspase-3 (Figure 3E–3G). Detailed quantitative analysis showed that the co-immunostaining cells of UBB $^{+1}$

with caspase-3 increased to 648.9 ± 18.9 cells/mm^2 in the ipsilateral striatum from 216.6 ± 21.8 cells/mm^2 in the contralateral side (Figure 3H). This result indicated that elevation of UBB $^{+1}$ expression and activation of caspase-3 occurred in the same cells in ischemia-injured brains.

Caspase-3 Inhibition Attenuated Ischemia-Induced Increases of UBB $^{+1}$ and BACE1 Proteins as well as the UBB $^{+1}$–BACE1 Protein Complex

To investigate whether activation of caspase-3 could regulate UBB $^{+1}$ generation in ischemic rat brain, we injected the specific caspase-3 inhibitor DEVD into the lateral ventricle of rat brains. DEVD significantly blocked activation of caspase-3 as seen by the marked reduction in the levels of the activated caspase-3 protein P20, a cleavage product of pro-caspase-3 P32 (Figure 4A). Under this condition, we found that DEVD treatment dramatically reduced the ischemia-induced protein level of UBB $^{+1}$ (Figure 4B and 4C). These data indicate that activation of caspase-3 is an event upstream of UBB $^{+1}$ formation in ischemia-injured brains.

Next, we examined the effect of caspase-3 inhibitor DEVD on BACE1 protein levels in this model. We found that increased BACE1 in ischemic striatum could be significantly reduced by DEVD treatment as compared with vehicle treatment (Figure 4D and 4E). We further performed immunoprecipitation to examine whether UBB $^{+1}$ and BACE1 could physically interact. Immunoprecipitation with an antibody against UBB $^{+1}$, followed by immunoblotting with an antibody against BACE1, revealed that a 65-kDa band corresponding to BACE1 was pulled down (Figure 4F), showing that UBB $^{+1}$ and BACE1 could
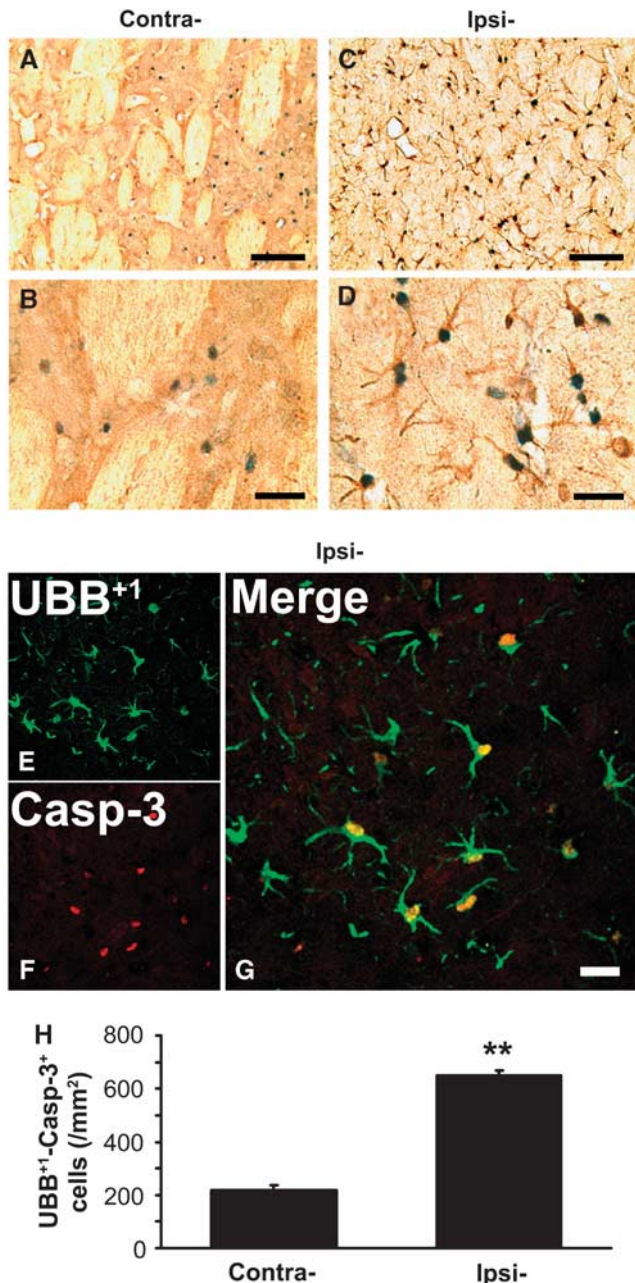
Figure 3 Colocalization of UBB^{+1} and activated caspase-3 in the ischemic striatum of rat brain. Brain sections from rats killed at 7 days after MCAO were examined by immunohistochemical double staining for UBB^{+1} (brown) and activated caspase-3 (blue) in the contralateral (Contra-) (**A**, **B**) and ipsilateral (Ipsi-) (**C**, **D**) striatum. These brain sections were also examined by confocal microscopy using antibodies specific for UBB^{+1} (**E**) and activated caspase-3 (**F**). The merged signals showed significant overlapping in ischemic striatum (**G**). Scale bars, (**A**, **C**): 100 μm; (**B**, **D**): 30 μm; (**G**): 20 μm. (**H**) Quantitative analysis showed that the number of UBB^{+1}–capsase-3^{+} cells increased significantly in the ischemic striatum at 7 days after MCAO (mean ± s.e.m.; **P < 0.01 versus contralateral; *n* = 3 to 4 in each group).

bind together and form a complex protein. The UBB^{+1} and BACE1 complex proteins were significantly higher in the ipsilateral striatum (vehicle) than in the contralateral side (control), as indicated in Figure 4F and 4G. Interestingly, DEVD treatment dramatically attenuated ischemia-induced increase of UBB^{+1} and BACE1 complex as compared with vehicle treatment. Furthermore, we performed reverse immunoprecipitation to confirm this interaction. The samples were immunoprecipitated with BACE1 antibody and immunoblotted with UBB^{+1} antibody. The results further showed that BACE1 and UBB^{+1} could bind to each other (Figure 4H). These complex proteins increased in the ischemia-injured striatum, which could be reduced by pretreatment with DEVD (Figure 4I).

Caspase-3 Inhibition Decreased the Number of UBB^{+1}, BACE1/Aβ Double-Stained Cells in Ischemic Striatum of Rat Brain

Since UBB^{+1} and BACE1 could bind together, we further examined their cellular localization by confocal microscopy. As shown in Figure 5A–5H, UBB^{+1}- and BACE1-positive stained cells in the ipsilateral striatum to ischemia (vehicle) were co-labeled with GFAP but not with NeuN, indicating that ischemia-induced increase of UBB^{+1} and BACE1 was mainly in the astrocytes.

Triple-labeled staining for UBB^{+1} (green), BACE1 (blue), and active caspase-3 (red), combined with confocal microscopy, revealed frequent colocalization of these signals within the same cells in the ischemic striatum (Figure 5I–5L). In the contralateral striatum (control), the immunofluorescent signals for active caspase-3 were barely detectable and the signals for UBB^{+1} and BACE1 were also weaker (data not shown). However, UBB^{+1}–BACE1 double-stained cells were significantly increased to 635.7 ± 37.8 cells/mm^2 in the ischemic striatum of vehicle-treated rats as compared with that in the control (259.9 ± 58.1 cells/mm^2). Moreover, DEVD treatment significantly reduced the number of UBB^{+1}–BACE1-stained cells (329.6 ± 31.0 cells/mm^2; Figure 5Q) in the ischemic striatum as compared with vehicle treatment. Furthermore, the number of triple labeled cells of UBB^{+1}, BACE1, and caspase-3 was dramatically increased in the ischemic striatum (380.3 ± 23.0 versus 151.5 ± 5.2 cells/mm^2 in the control) at 7 days after MCAO, whereas DEVD treatment significantly decreased the number of these triple stained cells to 172.6 ± 23.9 cells/mm^2 (Figure 5R).

We further found that UBB^{+1} (green), Aβ (blue), and active caspase-3 (red) also colocalized in the same cells in the ischemic striatum at 7 days after MCAO (Figure 5M–5P). The cell counting results showed that the number of UBB^{+1}–Aβ double-stained cells and UBB^{+1}–Aβ–caspase-3 triple-labeled cells in the ischemic striatum was significantly increased to 640.1 ± 21.1 and 434.8 ± 28.7 cells/mm^2, respectively, compared with 128.7 ± 22.3 and 93.2 ± 19.0 cells/mm^2, respectively in the controls. DEVD treatment dramatically decreased the number of UBB^{+1}–Aβ double-
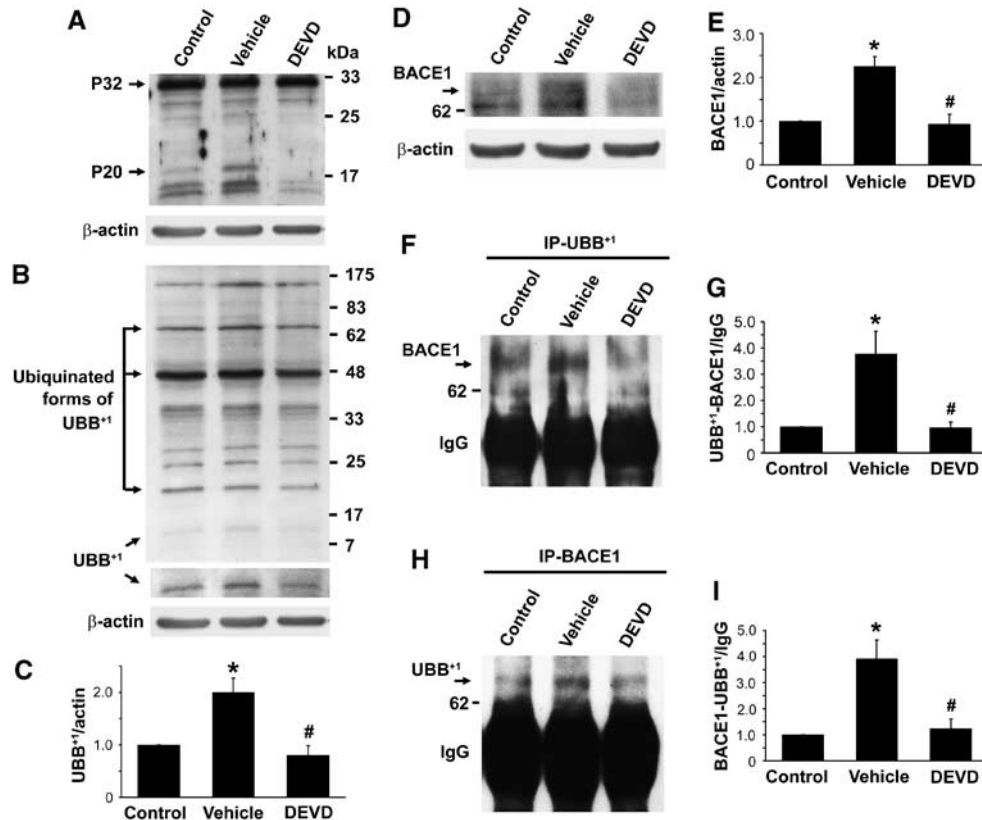
Figure 4 Changes in the expression of UBB^{+1} and BACE1 proteins, as well as the proteins of UBB^{+1}–BACE1 complex, in the ischemic striatum after caspase-3 inhibition. Treated rat brain lysates were prepared for western blot analysis with an antibody specific for caspase-3 (**A**). Pro-caspase-3 migrates as a 32-kDa protein (P32), while activated caspase-3 is recognized as P20. Western blot analysis of UBB^{+1} showed that the protein levels of UBB^{+1} in the ipsilateral striatum at 7 days after MCAO (vehicle) were significantly increased as compared with the protein levels in the contralateral side (control), while DEVD treatment significantly reduced ischemia-increased levels of UBB^{+1} (**B**, **C**). Western blot analysis of BACE1 showed that the protein levels of BACE1 in the vehicle-treated group were significantly increased in the ischemic striatum at 7 days after MCAO, and could be dramatically decreased in the DEVD-treated group (**D**, **E**). Striatal lysates were immunoprecipitated with anti-UBB^{+1} and immunoblotted with anti-BACE1 (**F**), and densitometric quantification of UBB^{+1}–BACE1-binding proteins levels showed that the UBB^{+1}–BACE1 complex proteins were robustly increased in the ipsilateral striatum at 7 days after MCAO as compared with those in the controls, and could be dramatically reduced by pretreatment with DEVD (**G**). Immunoprecipitation of striatal lysates with anti-BACE1 and then immunoblotting with anti-UBB^{+1} (**H**), and densitometric quantification of BACE1- and UBB^{+1}-binding protein levels (**I**) showed that the binding proteins were significantly increased in the ipsilateral striatum at 7 days after MCAO, and could be reduced in the DEVD-treated group (mean ± s.e.m.; *$P < 0.05$ versus control; #$P < 0.05$ versus vehicle; $n = 4$ to 5 in each group).

stained cells and UBB^{+1}–Aβ–caspase-3 triple-labeled cells to 155.3 ± 21.7 and 123.0 ± 2.5 cells/mm², respectively (Figure 5Q and 5R).

Discussion

In this study, we provide the first evidence that activation of caspases increases ischemia-induced generation of mutant ubiquitin UBB^{+1} in the brain, which may associate with increase in BACE1 stability and activity. We have reported here that a transient cerebral ischemia time-dependently increases the accumulation of UBB^{+1} and activation of caspase-3 in the brain. The time-course analysis has shown that caspase-3 activation occurs before UBB^{+1} generation. The caspase-3 inhibitor DEVD significantly reduced UBB^{+1} generation, while in-

hibiting caspase-3 activity and decreasing the amount of BACE1 in ischemic brains. Our results also show that UBB^{+1} can bind to BACE1, since both proteins can be immunoprecipitated (Figure 4). A caspase inhibitor can reduce the amount of BACE1–UBB^{+1}-binding proteins and the number of UBB^{+1}–BACE1 and UBB^{+1}–Aβ double-stained cells in ischemia-injured brains. Our results provide evidence for new biological effects of caspases and UPS regulation in the brain after ischemic stroke. The results present also provide new therapeutic targets to prevent further neurodegeneration in patients after stroke.

Consistent with a previous report, cerebral ischemia can increase the amount of UBB^{+1} in adult rodent brains (Yamashiro et al, 2007). Our present results show elevation of UBB^{+1} in ischemia-injured brains through activation of caspase-3. This is shown
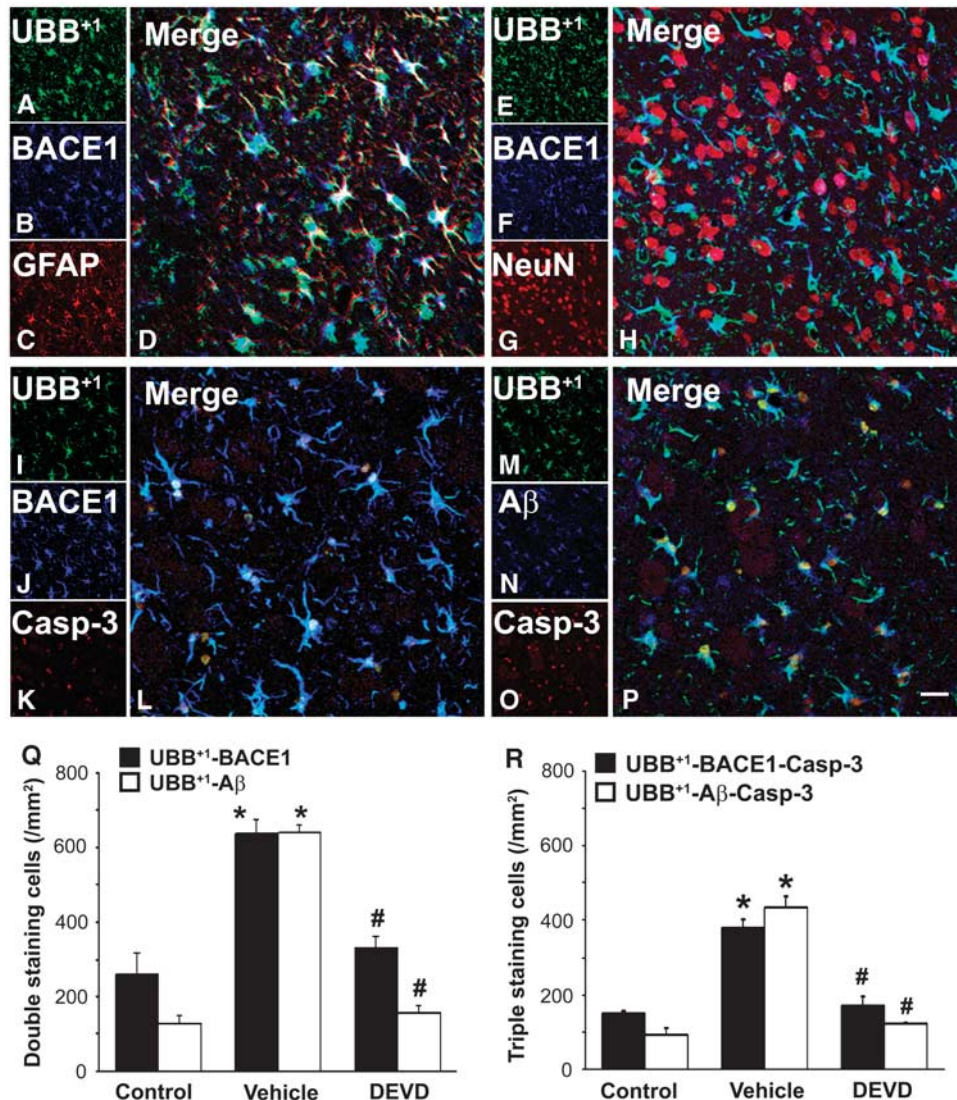
Figure 5 Caspase-3 inhibition reduced the number of UBB^{+1}, BACE1/Aβ double-stained cells in the ischemic striatum of rat brain. Confocal microscopy revealed that overlapping expression of UBB^{+1}/BACE1 mainly co-stained with GFAP (**A–D**), but not with NeuN (**E–H**), in the ischemic striatum. Confocal microscopy (**I–P**) showed cellular localization of UBB^{+1}, BACE1/Aβ, and active caspase-3 in the ipsilateral ischemic striatum at 7 days after MCAO. Scale bars: 20 μm. Statistical data (**Q**, **R**) show prominent increase of double- or triple-stained cells in the ischemic striatum of rats in the vehicle-treated group (vehicle) at 7 days after MCAO, and significant decrease in those in the DEVD-treated group (mean ± s.e.m.; *$P < 0.05$ versus control, #$P < 0.05$ versus vehicle; $n = 3$ to 4 in each group).

by the following pieces of evidence: (1) caspase-3 activation occurred earlier than UBB^{+1} elevation as indicated by our time-course analysis for increase of UBB^{+1} and caspase-3 (Figure 2); (2) confocal microscopic analysis showed cellular colocalization of UBB^{+1} with caspase-3 (Figure 3); and (3) DEVD, a specific caspase-3 inhibitor, blocked the ischemia-induced increase of UBB^{+1} in the brain (Figure 4). Therefore, we speculate that activation of caspase-3 is an event upstream of UBB^{+1} formation in ischemia-injured brains. However, the mechanism by which caspase-3 activation could induce UBB^{+1} elevation in ischemia-injured brain is still unknown, although it has been demonstrated that oxidative stress, which is often caused by ischemic neuronal

apoptosis, results in UBB^{+1} formation through molecular misreading and dinucleotide deletion in *UBB* gene transcription (Menendez-Benito *et al*, 2005).

In this study, we have found that UBB^{+1} may contribute to increased BACE1 activity through elevation of BACE1 stability in ischemia-injured brains. UBB^{+1} at physiological level can be a substrate to stimulate proteasome activity (Fischer *et al*, 2003; Lindsten *et al*, 2002). However, excessive UBB^{+1} becomes an endogenous proteasome inhibitor (van Tijn *et al*, 2007). Theoretically, once the protein excessively ligates with UBB^{+1}, it will become resistant to proteasome degradation. In this study, we have found that UBB^{+1} colocalizes with BACE1

in the cells (Figure 5) and UBB^{+1} can bind to BACE1 protein (Figure 4). More interestingly, cerebral ischemia simultaneously increases the binding of UBB^{+1} and BACE1 while also increasing the level of each free protein in the brain, which can be reduced by caspase-3 inhibitor (Figure 4). It should be noted that the ischemia-induced increase of UBB^{+1}–BACE1 binding was nearly twofold higher than increase in their free proteins, respectively. These data indicate that caspase-3 activation can increase BACE1 levels at least partly through reduction of BACE1 degradation through binding with UBB^{+1}. Previous studies have shown that active caspase-3 can increase BACE1 synthesis (Xiong *et al*, 2008) and increase BACE1 stability through increased cleavage of GGA3, a BACE1-trafficking molecule (Tesco *et al*, 2007). Furthermore, depletion of BACE1-trafficking protein GGA3 increases BACE1 activity and leads to Aβ accumulation in the thalamus and cortex (Hiltunen *et al*, 2009; Tesco *et al*, 2007). Combined with the present results, it becomes clear that caspase activation elevates BACE1 levels in ischemic brain through multiple regulations. Moreover, with this experimental model, we have shown increased BACE1 activity in ischemic brains by detection of the APP-C99 fragment, a C-terminal fragment of amyloid precursor protein (APP CTFs), and cleavage of APP by BACE1 (Tesco *et al*, 2007; Xiong *et al*, 2008). This study also clearly indicates that Aβ-positive cells co-stained with UBB^{+1} and/or caspase-3 (Figure 5). These cells were increased in number in the brain after ischemia, and this could be reduced by a caspase-3 inhibitor (Figure 5). Collectively, our results therefore suggest that BACE1 protein binding with UBB^{+1} retains its enzymatic activity, which is consistent with a previous report that β-galactosidase binding with mutant ubiquitin still has its own enzyme activity (Tank and True, 2009).

As mentioned above, caspase activation will induce UPS dysfunction through UBB^{+1} generation and increase Aβ generation through activation of BACE1 (Tesco *et al*, 2007; Xiong *et al*, 2008). Conversely, dysfunction of the UPS can cause neuronal death through stimulation of caspase activity. For example, in primary cultured neurons, inhibition of the proteasome triggers activation of caspase-mediated apoptotic pathway and results in neuronal death (Qiu *et al*, 2000). Aβ neurotoxicity occurs through increases of caspases. Interestingly, Aβ neurotoxicity also appears to be associated with UBB^{+1}-mediated proteasome inhibition (Song *et al*, 2003). Generally, UBB^{+1} at excessive levels can play endogenous inhibitory roles in proteasome degradation, thereby increasing neurotoxicity in the presence of Aβ through activation of caspase-medicated apoptotic pathways. Taking together, ischemia-induced activation of caspase-3 and elevation of UBB^{+1} may form a vicious cycle that potentially accelerates brain damage. Therefore, treatment with specific inhibitors of caspase-3, a key effector of the caspase-mediated apoptotic pathway, could potentially protect neurons against acute and chronic ischemic death through interruption of this cycle. The present findings should aid the exploration of novel therapies to prevent excessive accumulation of UBB^{+1} or Aβ in the brain, and lower the risk of Alzheimer's disease development after stroke.

Acknowledgements

Conflict of interest

The authors declare no conflict of interest.

References

Bence NF, Sampat RM, Kopito RR (2001) Impairment of the ubiquitin–proteasome system by protein aggregation. *Science* 292:1552–5

Chen J, Nagayama T, Jin K, Stetler RA, Zhu RL, Graham SH, Simon RP (1998) Induction of caspase-3-like protease may mediate delayed neuronal death in the hippocampus after transient cerebral ischemia. *J Neurosci* 18:4914–28

Ciechanover A, Brundin P (2003) The ubiquitin proteasome system in neurodegenerative diseases: sometimes the chicken, sometimes the egg. *Neuron* 40:427–46

De Strooper B, Saftig P, Craessaerts K, Vanderstichele H, Guhde G, Annaert W, Von Figura K, Van Leuven F (1998) Deficiency of presenilin-1 inhibits the normal cleavage of amyloid precursor protein. *Nature* 391:387–90

De Vrij FM, Sluijs JA, Gregori L, Fischer DF, Hermens WT, Goldgaber D, Verhaagen J, Van Leeuwen FW, Hol EM (2001) Mutant ubiquitin expressed in Alzheimer's disease causes neuronal death. *FASEB J* 15:2680–8

Fischer DF, De Vos RA, Van Dijk R, De Vrij FM, Proper EA, Sonnemans MA, Verhage MC, Sluijs JA, Hobo B, Zouambia M, Steur EN, Kamphorst W, Hol EM, Van Leeuwen FW (2003) Disease-specific accumulation of mutant ubiquitin as a marker for proteasomal dysfunction in the brain. *FASEB J* 17:2014–24

Hiltunen M, Makinen P, Peraniemi S, Sivenius J, van Groen T, Soininen H, Jolkkonen J (2009) Focal cerebral ischemia in rats alters APP processing and expression of Abeta peptide degrading enzymes in the thalamus. *Neurobiol Dis* 35:103–13

Hol EM, van Leeuwen FW, Fischer DF (2005) The proteasome in Alzheimer's disease and Parkinson's disease: lessons from ubiquitin B+1. *Trends Mol Med* 11:488–95

Hou SW, Wang YQ, Xu M, Shen DH, Wang JJ, Huang F, Yu Z, Sun FY (2008) Functional integration of newly generated neurons into striatum after cerebral ischemia in the adult rat brain. *Stroke* 39:2837–44

Kamikubo T, Hayashi T (1996) Changes in proteasome activity following transient ischemia. *Neurochem Int* 28:209–12

Keller JN, Huang FF, Zhu H, Yu J, Ho YS, Kindy TS (2000) Oxidative stress-associated impairment of proteasome activity during ischemia–reperfusion injury. *J Cereb Blood Flow Metab* 20:1467–73

Lam YA, Pickart CM, Alban A, Landon M, Jamieson C, Ramage R, Mayer RJ, Layfield R (2000) Inhibition of the ubiquitin–proteasome system in Alzheimer's disease. *Proc Natl Acad Sci USA* 97:9902–6

Leys D, Henon H, Mackowiak-Cordoliani MA, Pasquier F (2005) Poststroke dementia. *Lancet Neurol* 4:752–9

Lindsten K, de Vrij FM, Verhoef LG, Fischer DF, van Leeuwen FW, Hol EM, Masucci MG, Dantuma NP (2002) Mutant ubiquitin found in neurodegenerative disorders is a ubiquitin fusion degradation substrate that blocks proteasomal degradation. *J Cell Biol* 157:417–27

Lopez Salon M, Morelli L, Castano EM, Soto EF, Pasquini JM (2000) Defective ubiquitination of cerebral proteins in Alzheimer's disease. *J Neurosci Res* 62:302–10

Menendez-Benito V, Verhoef LG, Masucci MG, Dantuma NP (2005) Endoplasmic reticulum stress compromises the ubiquitin–proteasome system. *Hum Mol Genet* 14:2787–99

Morimoto T, Ide T, Ihara Y, Tamura A, Kirino T (1996) Transient ischemia depletes free ubiquitin in the gerbil hippocampal CA1 neurons. *Am J Pathol* 148:249–57

Qing H, Zhou W, Christensen MA, Sun X, Tong Y, Song W (2004) Degradation of BACE by the ubiquitin–proteasome pathway. *FASEB J* 18:1571–3

Qiu JH, Asai A, Chi S, Saito N, Hamada H, Kirino T (2000) Proteasome inhibitors induce cytochrome *c*–caspase-3-like protease-mediated apoptosis in cultured cortical neurons. *J Neurosci* 20:259–65

Qiu MH, Zhang R, Sun FY (2003) Enhancement of ischemia-induced tyrosine phosphorylation of Kv1.2 by vascular endothelial growth factor via activation of phosphatidylinositol 3-kinase. *J Neurochem* 87:1509–17

Sinha S, Anderson JP, Barbour R, Basi GS, Caccavello R, Davis D, Doan M, Dovey HF, Frigon N, Hong J, Jacobson-Croak K, Jewett N, Keim P, Knops J, Lieberburg I, Power M, Tan H, Tatsuno G, Tung J, Schenk D, Seubert P, Suomensaari SM, Wang S, Walker D, Zhao J, McConlogue L, John V (1999) Purification and cloning of amyloid precursor protein beta-secretase from human brain. *Nature* 402:537–40

Song S, Kim SY, Hong YM, Jo DG, Lee JY, Shim SM, Chung CW, Seo SJ, Yoo YJ, Koh JY, Lee MC, Yates AJ, Ichijo H, Jung YK (2003) Essential role of E2-25K/Hip-2 in mediating amyloid-beta neurotoxicity. *Mol Cell* 12:553–63

Tank EM, True HL (2009) Disease-associated mutant ubiquitin causes proteasomal impairment and enhances the toxicity of protein aggregates. *PLoS Genet* 5:e1000382

Tesco G, Koh YH, Kang EL, Cameron AN, Das S, Sena-Esteves M, Hiltunen M, Yang SH, Zhong Z, Shen Y, Simpkins JW, Tanzi RE (2007) Depletion of GGA3 stabilizes BACE and enhances beta-secretase activity. *Neuron* 54:721–37

van Leeuwen FW, de Kleijn DP, van den Hurk HH, Neubauer A, Sonnemans MA, Sluijs JA, Koycu S, Ramdjielal RD, Salehi A, Martens GJ, Grosveld FG, Peter J, Burbach H, Hol EM (1998) Frameshift mutants of beta amyloid precursor protein and ubiquitin-B in Alzheimer's and Down patients. *Science* 279:242–7

van Tijn P, de Vrij FM, Schuurman KG, Dantuma NP, Fischer DF, van Leeuwen FW, Hol EM (2007) Dose-dependent inhibition of proteasome activity by a mutant ubiquitin associated with neurodegenerative disease. *J Cell Sci* 120:1615–23

Vassar R, Bennett BD, Babu-Khan S, Kahn S, Mendiaz EA, Denis P, Teplow DB, Ross S, Amarante P, Loeloff R, Luo Y, Fisher S, Fuller J, Edenson S, Lile J, Jarosinski MA, Biere AL, Curran E, Burgess T, Louis JC, Collins F, Treanor J, Rogers G, Citron M (1999) Beta-secretase cleavage of Alzheimer's amyloid precursor protein by the transmembrane aspartic protease BACE. *Science* 286:735–41

Wang YQ, Guo X, Qiu MH, Feng XY, Sun FY (2007) VEGF overexpression enhances striatal neurogenesis in brain of adult rat after a transient middle cerebral artery occlusion. *J Neurosci Res* 85:73–82

Xiong M, Zhang T, Zhang LM, Lu SD, Huang YL, Sun FY (2008) Caspase inhibition attenuates accumulation of beta-amyloid by reducing beta-secretase production and activity in rat brains after stroke. *Neurobiol Dis* 32: 433–41

Yamashiro K, Liu R, Maeda M, Hattori N, Urabe T (2007) Induction and selective accumulation of mutant ubiquitin in CA1 pyramidal neurons after transient global ischemia. *Neuroscience* 147:71–9

Yan R, Bienkowski MJ, Shuck ME, Miao H, Tory MC, Pauley AM, Brashier JR, Stratman NC, Mathews WR, Buhl AE, Carter DB, Tomaselli AG, Parodi LA, Heinrikson RL, Gurney ME (1999) Membrane-anchored aspartyl protease with Alzheimer's disease beta-secretase activity. *Nature* 402:533–7

Zhang T, Pan BS, Zhao B, Zhang LM, Huang YL, Sun FY (2009) Exacerbation of poststroke dementia by type 2 diabetes is associated with synergistic increases of beta-secretase activation and beta-amyloid generation in rat brains. *Neuroscience* 161:1045–56